

# The determination of the DNA sequence specificity of bleomycin-induced abasic sites

Jon K. Chen<sup>1</sup> · Vincent Murray<sup>1</sup>

Received: 29 December 2015 / Accepted: 22 February 2016 / Published online: 3 March 2016  
© SBIC 2016

**Abstract** The DNA sequence specificity of the cancer chemotherapeutic agent, bleomycin, was determined with high precision in purified plasmid DNA using an improved technique. This improved technique involved the labelling of the 5'- and 3'-ends of DNA with different fluorescent tags, followed by simultaneous cleavage by bleomycin and capillary electrophoresis with laser-induced fluorescence. This permitted the determination of bleomycin cleavage specificity with high accuracy since end-label bias was greatly reduced. Bleomycin produces single- and double-strand breaks, abasic sites and other base damage in DNA. This high-precision method was utilised to elucidate, for the first time, the DNA sequence specificity of bleomycin-induced DNA damage at abasic sites. This was accomplished using endonuclease IV that cleaves DNA at abasic sites after bleomycin damage. It was found that bleomycin-induced abasic sites formed at 5'-GC and 5'-GT sites while bleomycin-induced phosphodiester strand breaks formed mainly at 5'-GT dinucleotides. Since bleomycin-induced abasic sites are produced in the absence of molecular oxygen, this difference in DNA sequence specificity could be important in hypoxic tumour cells.

**Keywords** Abasic DNA damage, bleomycin · Cleavage sites · DNA sequence specificity · End-label bias · Endonuclease IV

## Abbreviations

CE-LIF	Capillary electrophoresis with laser-induced fluorescence
dNTP	Deoxynucleotide triphosphates
FAM-dUTP	Aminoallyl-dUTP-6-FAM
Rb1	Human retinoblastoma 1 gene

## Introduction

Bleomycin is a cancer chemotherapeutic agent that is currently employed in the treatment of Hodgkin's lymphoma, squamous cell carcinoma and testicular cancer [1, 2]. Bleomycin is a natural product glycopeptide antibiotic derived from *Streptomyces verticillus* [3]. The anti-tumour activity of bleomycin is thought to derive from its ability to cause single- and double-strand breaks and base damage in DNA [4–6].

Bleomycin is administered intravenously in a metal-free form [7]. Cu(II) from blood plasma binds to intravenous bleomycin to form bleomycin–Cu(II) and is transported into the cell [6]. Once inside the cell, the bleomycin–Cu(II) complex is reduced to bleomycin–Cu(I) which in turn is displaced by Fe(II). The subsequent reaction mechanism involves the oxidation of the chelated divalent cation, Fe(II) to Fe(III), and generation of a free radical at the 4'-carbon of the deoxyribose [6–11]. If oxygen is present, phosphodiester cleavage occurs with production of a 5'-phosphate, 3'-phosphoglycolate and release of base propenal that destroys the nucleotide at the cleavage site. If oxygen is absent, a pyrimidine base is lost from the DNA to produce an abasic site [12].

Bleomycin cleaves DNA with sequence specificity, mainly at 5'-GT dinucleotides. The DNA sequence specificity of bleomycin has mainly been determined in purified

✉ Vincent Murray  
v.murray@unsw.edu.au

<sup>1</sup> School of Biotechnology and Biomolecular Sciences, University of New South Wales, Sydney, NSW 2052, Australia

plasmid DNA sequences [13–21]. The bleomycin sequence specificity has also been elucidated in human cellular DNA [22–28]. Recently, we expanded the DNA sequence specificity of bleomycin using next-generation sequencing and found that in human cells bleomycin preferentially cleaves at 5'-RTGT\*AY where R is a purine (G or A), Y is a pyrimidine (T or C), and T\* is the cleavage site [29]. Bleomycin has been shown to cleave in the linker region of nucleosomes [22, 29–32].

For purified plasmid DNA, the current method for determining the sequence specificity of bleomycin involves end-labelled DNA [21, 28, 33–38]. The fluorescently end-labelled DNA is cleaved by bleomycin and subjected to capillary electrophoresis with laser-induced fluorescence (CE-LIF) alongside DNA sequencing reactions as molecular weight size markers. Hence, the precise sites of bleomycin cleavage can be determined and the degree of cleavage evaluated by quantification of fluorescence intensity [33, 35, 38].

In this paper, we determined the sequence specificity of bleomycin DNA damage with a high level of precision in a defined plasmid construct. In the first aim of the current study, we attempted to overcome previous problems with DNA sequence specificity measurements, especially end-label bias [34, 35, 38–42]. End-label bias is a difficult problem to overcome because in an end-labelled DNA fragment, if there are two cleavage events in a single DNA molecule, then only the cleavage site closest to the labelled end is observed [35]. This results in the apparent cleavage sites being shifted towards the labelled end of the DNA fragment. Previous attempts to remove end-label bias using an algorithm have only been partially successful, especially in higher frequency cleavage experiments [34, 35]. In this paper, we employed DNA fragments labelled with a different fluorescent dye at either the 5'- or 3'-end, and attempted to overcome the end-label bias problem by simultaneous cleavage of these dually labelled DNA fragments.

The second major aim of this study was to determine for the first time, the DNA sequence specificity of bleomycin-induced abasic cleavage. The normal method for analysing bleomycin strand breaks involves capillary electrophoresis; however, this method does not reveal bleomycin abasic site DNA damage. Endonuclease IV has several major activities including the ability to cleave phosphodiester linkages at abasic sites [43, 44]. This activity allows, for the first time, the determination of the DNA sequence specificity at bleomycin-induced abasic sites and a comparison with direct bleomycin-induced phosphodiester cleavage. The use of endonuclease IV permits the cleavage at bleomycin-produced abasic sites and after capillary electrophoresis, the elucidation of the bleomycin DNA sequence selectivity at these abasic sites.

## Materials and methods

### Materials

Bleomycin was obtained from Bristol Laboratories under the trade name Blenoxane. The clinical preparation, Blenoxane, consisted of 70 % bleomycin A<sub>2</sub> and 30 % bleomycin B<sub>2</sub>. The enzymes exonuclease I, shrimp alkaline phosphatase, Klenow fragment DNA polymerase and endonuclease IV were obtained from New England Biolabs. AmpliTaq<sup>®</sup> DNA polymerase was supplied by Life Technologies. The deoxynucleotide triphosphates (dNTP) were purchased from New England Biolabs; and the fluorescently labelled aminoallyl-dUTP-6-FAM (FAM-dUTP) from Jena Biosciences, Germany.

The HPLC-purified oligonucleotides REV2 (5'-ATTGTG AGCGGATAAC-3') and SEQ (5'-TCCCAGTCACGA CGT-3') were supplied by Invitrogen. The PET-labelled version of the SEQ oligonucleotide was obtained from Applied Biosystems.

### Preparation of end-labelled DNA fragments

The pUC19-based plasmid, T7Rb1G10, was constructed by introducing a section of the human retinoblastoma 1 (Rb1) gene promoter into the T7G10 plasmid [45]. A section of the human retinoblastoma 1 (Rb1) gene promoter (bp position 48303698–48303746 on chromosome 13 in the GRCh38/hg38 human DNA sequence assembly) was amplified by PCR and inserted into the *SacI* site of the plasmid using conventional methods. The T7Rb1G10 plasmid contained seven telomeric sequence repeats (T7), the Rb1 gene promoter and a sequence of ten consecutive guanines (G10) (Fig. 1).

A section of the T7Rb1G10 construct was amplified by PCR with the REV2 and SEQ primers to generate the target DNA sequences for bleomycin damage experiments. Each reaction consisted of approximately 3.5 ng of the plasmid DNA; 5 pmol REV2 and SEQ primer, each; 16.6 mM (NH<sub>4</sub>)<sub>2</sub>SO<sub>4</sub>; 67 mM Tris–HCl, pH 8.8; 6.7 mM MgCl<sub>2</sub>; and 1 U of AmpliTaq<sup>®</sup> DNA polymerase. The reaction mixtures were subjected to thermal cycling at 95 °C for 5 min; followed by 25 cycles of 95 °C for 45 s, 55 °C for 1 min, 72 °C for 2 min; and finally a single cycle of 72 °C for 10 min.

The PCR products were labelled at the 3'-end with FAM using the previously described method [34, 46]. Prior to the labelling procedure, the PCR precursors were removed by Exo-SAP. To 10 µL of the PCR product, 2 µL of Exo-SAP mix (67 mM Glycine-KOH, pH 9.5; 6.7 mM MgCl<sub>2</sub>; 10 mM β-mercaptoethanol; 2 U exonuclease I; 0.1 U shrimp alkaline phosphatase) was added. The samples were treated at 37 °C for 30 min, followed by 80 °C for 15 min to inactivate

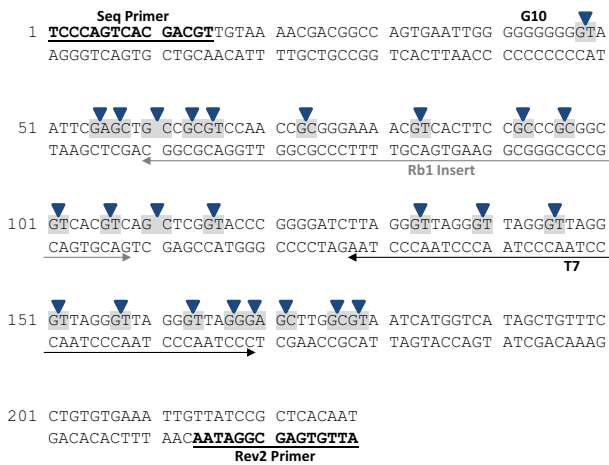


**Fig. 1** The DNA sequence of the T7Rb1G10 plasmid construct used in this study. This DNA sequence was amplified and fluorescently labelled for bleomycin cleavage assays. This construct contained the telomeric repeat sequence (labelled T7) and a consecutive run of ten guanines (G10). In addition, a sequence derived from the promoter region of the retinoblastoma 1 gene was present in the construct (labelled Rb1). Bleomycin cleavage sites observed in this study are indicated on the sequence with *blue arrows*. The top DNA strand is written 5' → 3' and the bottom strand is 3' → 5'. The Rev2 and Seq oligonucleotide primers are indicated in *bold* and *underlined*

the Exo-SAP mix. Following that, 8  $\mu$ L of the labelling mix (25 mM Tris–HCl, pH 7.9; 125 mM NaCl; 25 mM MgCl<sub>2</sub>; 2.5 mM dithiothreitol; 125  $\mu$ M of dATP, dCTP, and dGTP; 6.25  $\mu$ M FAM-dUTP; and 0.5 U Klenow fragment) was added to each of these Exo-SAP-treated samples. The labelling procedure was allowed to proceed at 37 °C for 30 min, followed by a heat inactivation step at 75 °C for 15 min.

A total of ten PCRs were performed to generate a large batch of labelled products that were purified by native polyacrylamide gel electrophoresis. Bands containing the labelled DNA were excised and recovered from the gel by soaking in 0.3 M sodium acetate at 37 °C overnight. The DNA was then concentrated by ethanol precipitation and redissolved in 25  $\mu$ L TE (10 mM Tris–HCl, pH 8.8; 0.1 mM EDTA) buffer.

Preparation of the 5'-end (PET)-labelled fragments was carried out by substitution of the SEQ primer with a PET pre-labelled SEQ primer during PCR. They were then purified by native polyacrylamide gel electrophoresis (as above) and reconstituted in 40  $\mu$ L TE (10 mM Tris–HCl, pH 8.8; 0.1 mM EDTA) buffer. Maxam and Gilbert G + A sequencing reactions as molecular weight size markers were performed as previously described [34].

### Bleomycin cleavage assays

Simultaneous bleomycin cleavage assays were performed in 10  $\mu$ L reactions that consisted of approximately 6 ng of

the 3'-end FAM and 5'-end PET-labelled T7Rb1G10 construct; and 720 ng purified chicken DNA as a carrier. Equimolar amounts of FeSO<sub>4</sub> and bleomycin were added to the DNA, to final concentrations ranging from 0.03–0.24 mM. The reactions were incubated at 37 °C for 30 min. The treated DNA samples were then recovered by ethanol precipitation and redissolved in 10  $\mu$ L TE (10 mM Tris–HCl, pH 8.8; 0.1 mM EDTA) buffer.

### Endonuclease IV treatment on bleomycin-damaged DNA

Bleomycin-damaged samples were further treated with endonuclease IV to induce additional breaks in the DNA at bleomycin-induced abasic lesion sites. In a total volume of 10  $\mu$ L, an exonuclease IV treatment consisted of 5  $\mu$ L of the bleomycin damage sample, 1  $\times$  NEBuffer 3 (50 mM Tris–HCl, pH 7.9, 100 mM NaCl, 10 mM MgCl<sub>2</sub>, and 1 mM DTT), and 5 U endonuclease IV. The reaction was allowed to proceed at 37 °C for 1 h, after which the DNA was recovered by ethanol precipitation and redissolved in 5  $\mu$ L of 10 mM Tris–HCl, pH 8.8; 0.1 mM EDTA solution.

### Analysis of cleavage fragments

Aliquots of 1–2  $\mu$ L of the treated samples were submitted to the Ramaciotti Centre for Genomics for fragment analysis. The cleavage fragments were resolved using the ABI 3730 automated capillary sequencer. The resulting data were then processed using Genemapper<sup>®</sup> (Applied Biosystems) v3.7 software. The identity of the peaks corresponding to bleomycin cleavage fragments were determined by comparison with the G + A sequencing ladder. The peaks were then quantified by their area under the curve and expressed as percentages over sum of all fragments. An algorithmic correction procedure was applied to the data to compensate for end-label bias [34, 35]. The resulting corrected peak profiles were averaged over three independent repeat experiments. To determine the sequence specificity for a particular strand, the averaged 3'- and 5'-end data were amalgamated.

## Results

### Bleomycin DNA cleavage

Sections of the T7Rb1G10 plasmid (Fig. 1) were amplified by PCR and fluorescently labelled (separately) at the 3'- and 5'-ends with FAM and PET, respectively. The 3'-FAM and 5'-PET PCR products were then combined and subjected to the bleomycin cleavage reaction. This allowed the simultaneous observation of bleomycin cleavage using

DNA strands labelled at both ends of the molecule. The DNA cleavage reactions were performed with bleomycin at concentrations ranging from 0.03 to 0.24 mM, supplemented with equimolar concentrations of  $\text{Fe}^{2+}$ . The resulting cleavage fragments were then resolved by CE-LIF.

Electropherograms showed that cleavage in the no bleomycin control samples were very low (Fig. 2a, c), except for artefact bands at sizes greater than 170 bp. Further treatment of the no bleomycin controls with endonuclease IV did not produce any further breakage in the DNA (Fig. 2b, d), except for an artefact band at 30 bp.

Bleomycin treatment produced breaks in the T7Rb1G10-labelled fragments and electropherograms showed numerous peaks corresponding to different cleavage sites on the DNA (Fig. 3a, c). In this bleomycin reaction, the supplemented ferrous ions are oxidised to ferric ions and this is the driving force in the reaction that leads to DNA strand breakage and DNA base damage. The naturally occurring product of *Streptomyces verticillus*, bleomycin, has harnessed this oxidation reaction to target and damage specific sequences of DNA. As expected, increasing the concentration of bleomycin (and equimolar  $\text{Fe}^{2+}$ ) was reflected in the overall increase in the fluorescent intensity of the cleavage peaks and decrease in the full length peak corresponding to the intact DNA (data not shown). Resolving the 3'- (FAM, blue)- and 5'-end (PET, red)-labelled fragments revealed electropherograms with similar bleomycin cleavage profiles that mirrored each other.

### The effect of endonuclease IV

The intensity of the bleomycin cleavage peaks increased after further treatment of the bleomycin-damaged samples with endonuclease IV, while the intensity of the full length product at 228 bp decreased (Fig. 3b, d). This was observed for both the 3'- and 5'-end-labelled fragments. As previously found, the cleavage peaks corresponding to the 5'-end-labelled fragments shifted in their apparent fragment size after endonuclease IV treatment [36]. This was due to the anomalous migration of 3'-phosphoglycolate ends produced by bleomycin that are converted to 3'-hydroxyl ends by endonuclease IV treatment [36]. The amount of endonuclease IV utilised (5U) converted all of the 3'-phosphoglycolate ends (produced by bleomycin) to 3'-hydroxyl ends—this can be monitored on an electropherogram (Fig. 3) because a DNA fragment with a 3'-phosphoglycolate end has different mobility to a fragment with a 3'-hydroxyl end. Xu et al. [44] found that endonuclease IV cleaved 3'-phosphoglycolate sites as efficiently as it cleaved abasic sites. Thus, since all the 3'-phosphoglycolate ends have been converted, it can be assumed that all the abasic sites have also been cleaved.

The identity of the cleavage peaks were determined by alignment of the peak profile with DNA sequencing ladders generated from the Maxam–Gilbert G + A method (Fig. 4). As expected, bleomycin cleavage occurred primarily at 5'-GT and 5'-GC sequences (Fig. 1).

The frequency of bleomycin cleavage for each site was determined by quantification of the area under the corresponding peaks. A correction algorithm was applied to the cleavage profiles to correct for the end-label bias that occurs due to two or more cleavage events on a single DNA fragment [34, 35]. The frequency for each cleavage site was expressed as a percentage of the total area of all of the peaks. The cleavage profile of T7Rb1G10 after treatment with bleomycin is shown in Fig. 5. The profile of the 5'-end (PET)-labelled fragments was flipped vertically for comparison with its horizontally-flipped 3'-end (FAM)-labelled counterpart (Fig. 5a). Both cleavage profiles appeared similar after correction for their respective end-label biases. For the bleomycin-damaged samples that were further treated with endonuclease IV, both the profiles of the 3'- and 5'-end-labelled fragments also appear to be similar (Fig. 5b).

The pre- and post-endonuclease IV treatment bleomycin cleavage sites are shown in Fig. 6 (and Tables 1, 2). There was an increase in the bleomycin cleavage intensity after endonuclease IV treatment (Fig. 6). Interestingly, there was a change in the bleomycin cleavage profile after endonuclease IV treatment. A greater increase was observed in several bleomycin cleavage sites, relative to others. For instance, the cleavage intensity of the site at bp 84 increased approximately tenfold (Table 3). In addition, the site at bp 102, which was ranked thirteenth among the cleavage sites, saw an increase by 8.8-fold to become the third most frequently cleaved site (Tables 1, 2). The site at bp 74 that contained a 5'-GC dinucleotide, was ranked eleventh and moved to fifth after endonuclease IV treatment. In contrast, the site at bp 180, while being one of the top bleomycin cleavage site, only saw an increase of 2.9-fold after endonuclease IV treatment. Overall, the intensity of the peaks increased by a factor ranging from 1.7- to 10.2-fold, with an average of 4.5-fold.

Linear regression plots were utilised to investigate the correlation of the bleomycin cleavage sites as determined by 5'- or 3'-end labelling (Fig. 7). The effect of the end-label bias correction algorithm can be seen in panels a, c and e compared with panels b, d and f where the  $R^2$  values increased from 0.33–0.75 to 0.95–0.96. This showed that the correction algorithm was working as expected.

The effect of simultaneous vs separate non-simultaneous bleomycin cleavage of 5'- or 3'-end labelling can be observed in a comparison of panels a and b with c and d. The  $R^2$  values for simultaneous cleavage is higher comparing panel c with a; and the  $R^2$  values are very similar in panels b

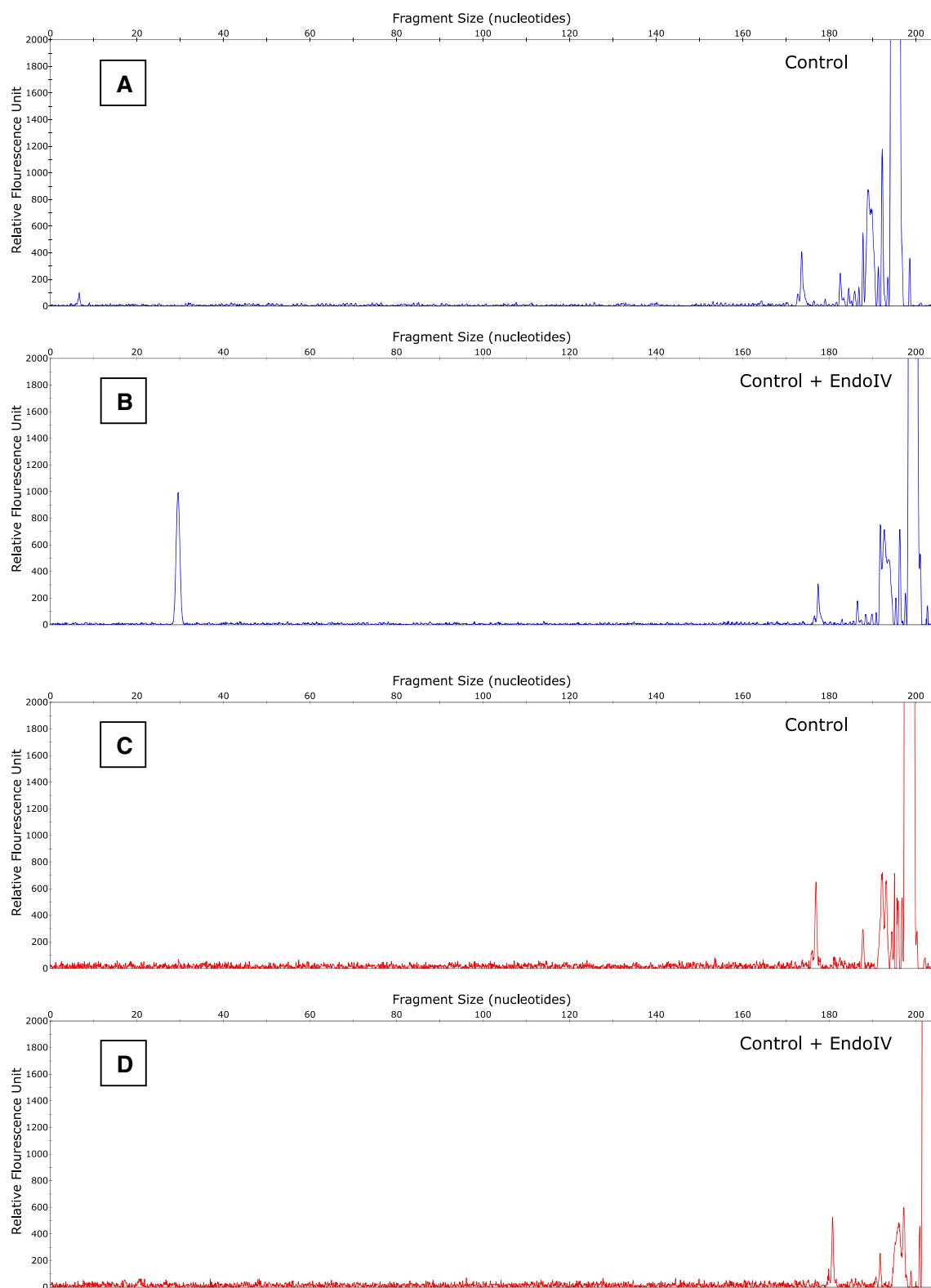
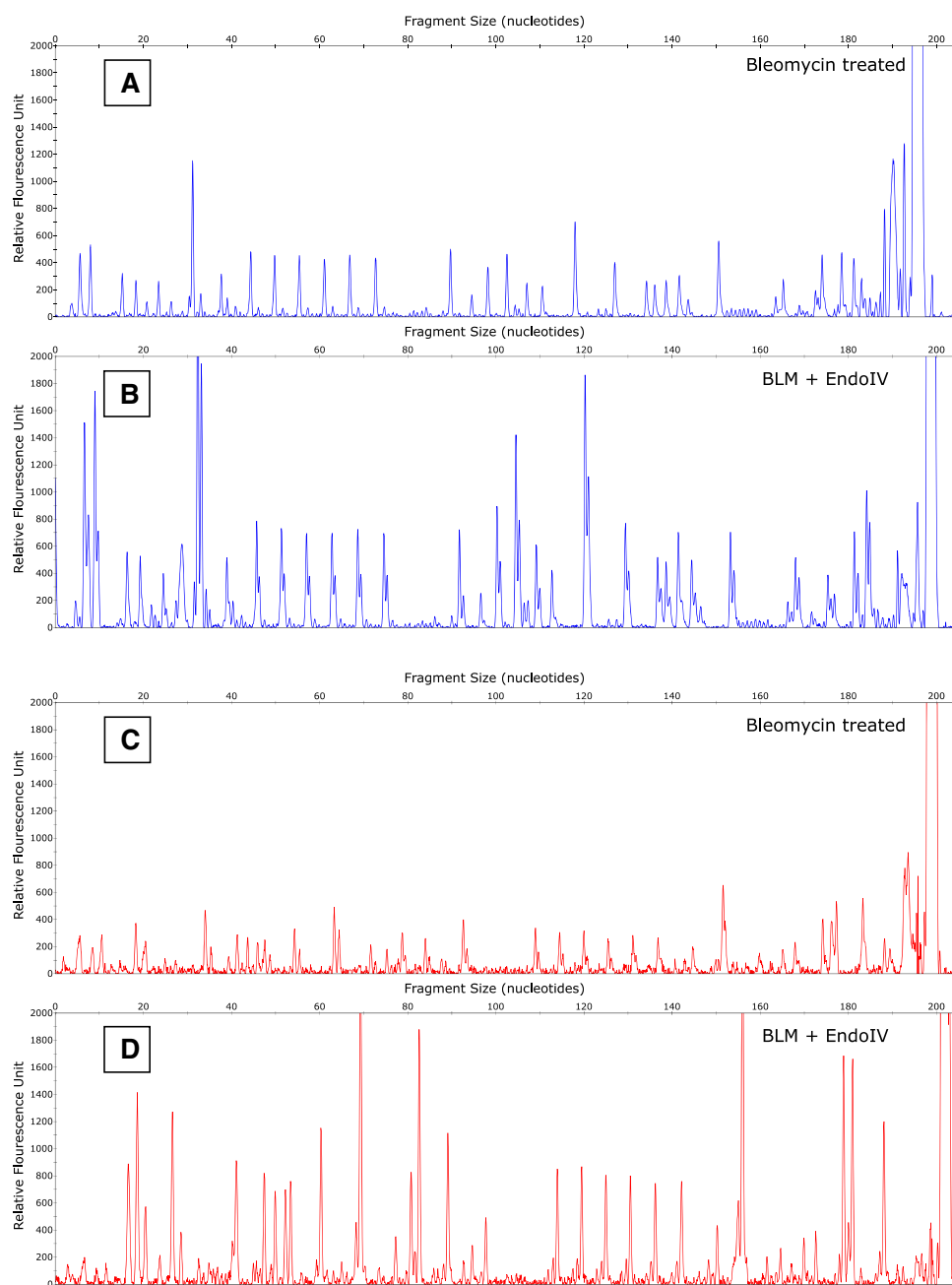


**Fig. 2** Fragment analysis of the labelled DNA construct in the absence of bleomycin treatment. The electropherograms show the full length peak corresponding to the *PvuII* site in the T7Rb1G10 DNA construct at approximately 200 bp. The trace of the 3'-labelled DNA fragment is in *blue* (**a**, **b**); while the 5'-labelled DNA fragment is in

*red* (**c**, **d**). The controls were either treated with endonuclease IV (**b**, **d**) or not treated with endonuclease IV (**a**, **c**). A large intensity peak at 30 bp and several smaller intensity peaks observed in the electropherograms were designated as artefacts and were discarded during the analysis of bleomycin cleavage assays

**Fig. 3** Fragment analysis of bleomycin cleavage with T7Rb1G10 DNA. The electropherograms reveal the bleomycin cleavage profiles with the two end-labelled constructs. Electropherogram traces in *blue* show the profile of fragments labelled at the 3'-end with FAM (**a, b**); and *red* traces represent fragments labelled at the 5'-end with PET (**c, d**). The samples were either treated with endonuclease IV (**b, d**) or not treated with endonuclease IV (**a, c**)



and d. Comparing the slopes of the best fitting straight lines, the simultaneous values are close to one in panels d and f (1.090 and 1.015) while the non-simultaneous bleomycin cleavage in panel b was much lower (0.635). This indicates that simultaneous bleomycin cleavage produced similar damage on both labelled strands while this was more difficult to achieve with separate non-simultaneous bleomycin cleavage. The  $R^2$  value in panel e is lower because there is a higher level of bleomycin damage that leads to a higher level of end-label bias and hence a lower  $R^2$  value.

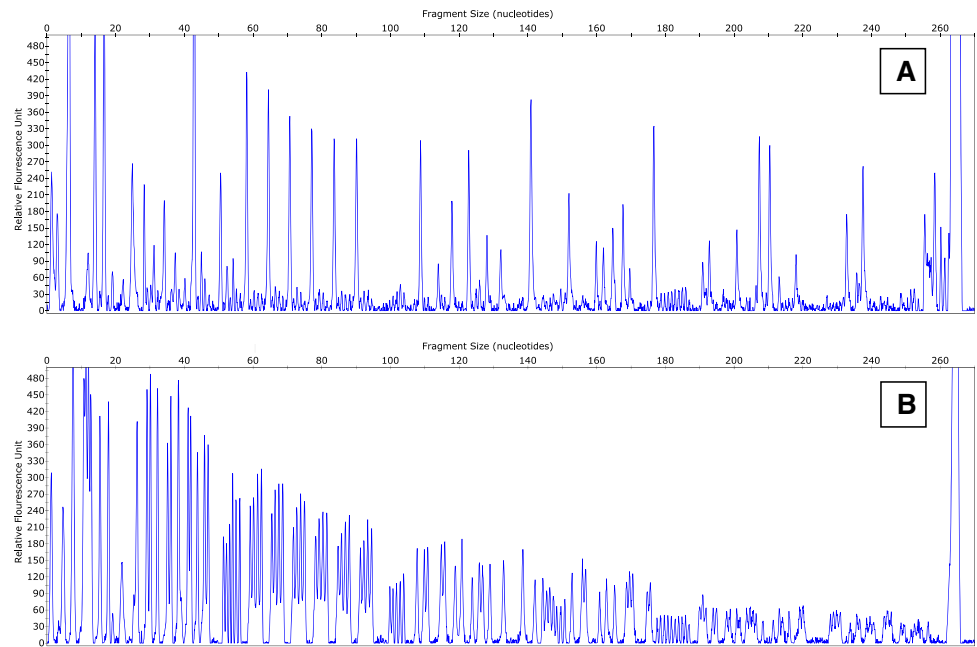
The highest  $R^2$  value, 0.964, was found in panel f and suggests that simultaneous bleomycin cleavage, with

endonuclease IV treatment and application of the correction algorithm produces the highest correlation of 5'- or 3'-end labelling. This further implies that these conditions produced the most accurate bleomycin cleavage profile.

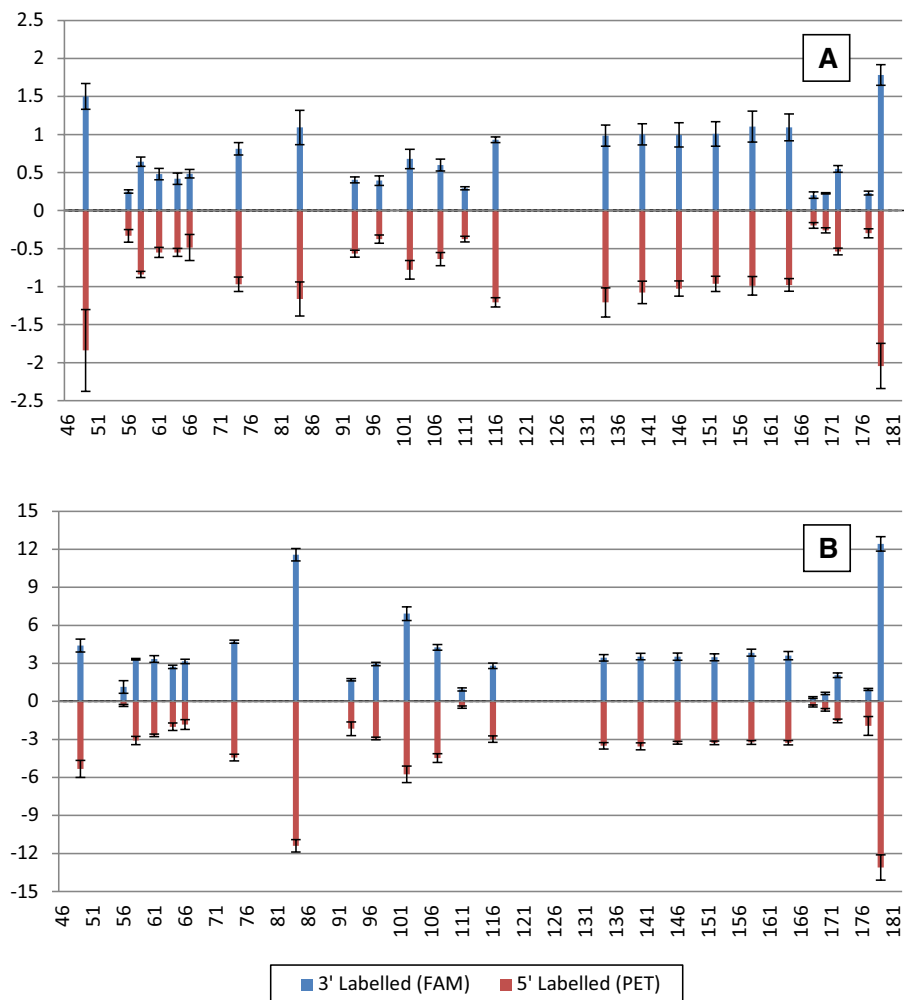
### The DNA sequence specificity of bleomycin cleavage with the T7Rb1G10 plasmid

Table 1 shows the DNA sequences at the 20 most intense bleomycin cleavage sites before endonuclease IV treatment. Note that the 5'- and 3'-end-labelled data have been combined in Table 1 and subsequent tables. The

**Fig. 4** The precise identification of bleomycin cleavage sites using DNA sequencing reactions. The T7Rb1G10 DNA labelled at the 3'-end with FAM was subjected to Maxam–Gilbert G + A sequencing. The peak profile observed corresponds to G and A nucleotides found in the DNA sequence (b). This sequencing ladder was aligned to bleomycin-treated profiles (a) to identify the precise DNA sequence of the bleomycin cleavage sites



**Fig. 5** Bleomycin cleavage profile of the T7Rb1G10 construct, before and after treatment with endonuclease IV. The graphs show the intensity of bleomycin cleavage before endonuclease IV treatment (a) at different sites in the construct, as observed from the 3'-end (blue) and the 5'-end (red). The profiles of the 5'-end (red)-labelled fragments have been flipped vertically for comparison with its horizontally-flipped 3'-end (blue)-labelled counterpart. The intensity of bleomycin cleavage after endonuclease IV treatment is shown (b). The profiles have been algorithmically corrected for end-label bias. Note the change in the y-axis scale in (b). Error bars indicate the standard deviation of the mean



**Fig. 6** Intensity of bleomycin cleavage sites before and after treatment with endonuclease IV. The percentage bleomycin cleavage is shown for the bleomycin damage sites. The intensity after treatment with endonuclease IV (*red*) is compared with the non-endonuclease IV-treated bleomycin samples (*blue*). Error bars indicate the standard deviation of the mean

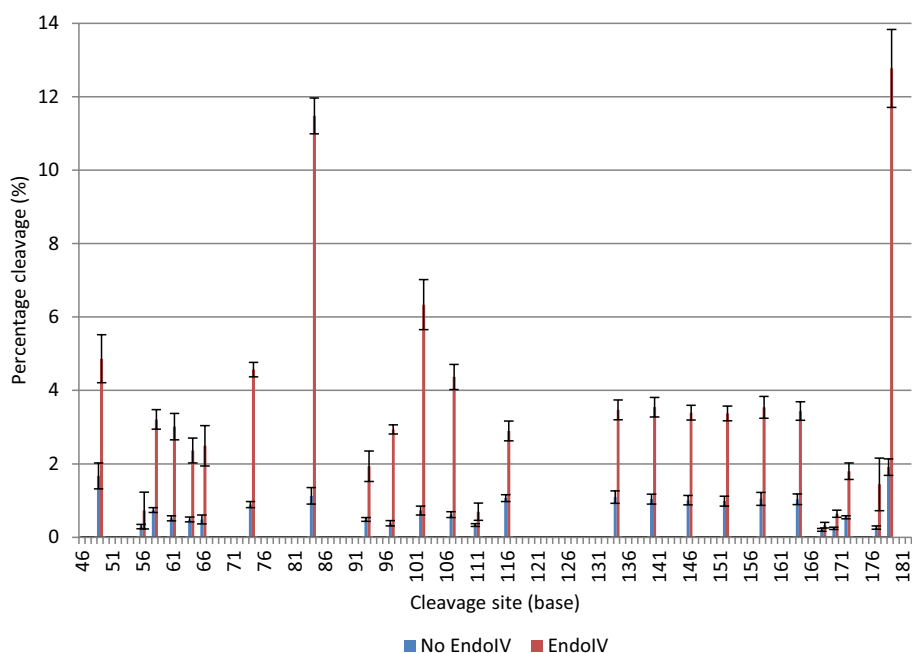


**Table 1** The DNA sequences of the 20 most intense bleomycin cleavage sites before endonuclease IV treatment using the T7Rb1G10 plasmid

Base	% cleavage	Sequence
179	1.91	TGGC <b>GT</b> AATC
49	1.67	GGGG <b>GT</b> AATT
84	1.13	AAAC <b>GT</b> CACT
134	1.10	TAGG <b>GT</b> TAGG
116	1.07	CTCG <b>GT</b> ACCC
158	1.05	TAGG <b>GT</b> TAGG
140	1.04	TAGG <b>GT</b> TAGG
164	1.04	TAGG <b>GT</b> TAGG
146	1.01	TAGG <b>GT</b> TAGG
152	0.99	TAGG <b>GT</b> TAGG
74	0.89	AACC <b>GC</b> GGGA
58	0.74	TCGA <b>GC</b> TGCC
102	0.73	CGGC <b>GT</b> CACG
107	0.62	TCAC <b>GT</b> CAGC
172	0.54	GGGA <b>GC</b> TTGG
61	0.51	AGCT <b>GC</b> CGCG
93	0.49	TTCC <b>GC</b> CCGC
64	0.49	TGCC <b>GC</b> GTCC
66	0.49	CCGC <b>GT</b> CCAA
97	0.38	GCCC <b>GC</b> GGCG

Bleomycin cleavage sites on the T7Rb1G10 plasmid were sorted based on their observed frequency of occurrence. The 5'- and 3'-end-labelled data have been combined. The dinucleotide sequence where the breakage occurred is in bold. In addition, the tetranucleotide sequences flanking the cleavage site are listed in the table

**Table 2** The DNA sequences of the 20 most intense bleomycin cleavage sites after endonuclease IV treatment

Base	% cleavage	Sequence
179	12.77	TGGC <b>GT</b> AATC
84	11.48	AAAC <b>GT</b> CACT
102	6.34	CGGC <b>GT</b> CACG
49	4.86	GGGG <b>GT</b> AATT
74	4.57	AACC <b>GC</b> GGGA
107	4.37	TCAC <b>GT</b> CAGC
140	3.54	TAGG <b>GT</b> TAGG
158	3.54	TAGG <b>GT</b> TAGG
134	3.47	TAGG <b>GT</b> TAGG
164	3.44	TAGG <b>GT</b> TAGG
146	3.39	TAGG <b>GT</b> TAGG
152	3.37	TAGG <b>GT</b> TAGG
58	3.21	TCGA <b>GC</b> TGCC
61	3.01	AGCT <b>GC</b> CGCG
97	2.94	GCCC <b>GC</b> GGCG
116	2.89	CTCG <b>GT</b> ACCC
66	2.49	CCGC <b>GT</b> CCAA
64	2.36	TGCC <b>GC</b> GTCC
93	1.93	TTCC <b>GC</b> CCGC
172	1.80	GGGA <b>GC</b> TTGG

Bleomycin cleavage sites on the T7Rb1G10 plasmid were sorted based on their observed frequency of occurrence. The 5'- and 3'-end-labelled data have been combined. The dinucleotide sequence where the breakage occurred is in bold and the tetranucleotide sequences flanking the cleavage site are listed in the table



**Table 3** The DNA sequences of the bleomycin cleavage sites with the 20 highest ratios after/before endonuclease IV treatment

Base	Ratio	Sequence		
84	10.18	AAAC	<b>GT</b>	CACT
102	8.70	CGGC	<b>GT</b>	CACG
97	7.64	GCCC	<b>GC</b>	GGCG
107	7.07	TCAC	<b>GT</b>	CAGC
179	6.68	TGGC	<b>GT</b>	AATC
61	5.85	AGCT	<b>GC</b>	CGCG
177	5.46	CTTG	<b>GC</b>	GTAA
66	5.14	CCGC	<b>GT</b>	CCAA
74	5.13	AACC	<b>GC</b>	GGGA
64	4.87	TGCC	<b>GC</b>	GTCC
58	4.33	TCGA	<b>GC</b>	TGCC
93	3.98	TTCC	<b>GC</b>	CCGC
152	3.42	TAGG	<b>GT</b>	TAGG
140	3.41	TAGG	<b>GT</b>	TAGG
158	3.38	TAGG	<b>GT</b>	TAGG
146	3.36	TAGG	<b>GT</b>	TAGG
164	3.32	TAGG	<b>GT</b>	TAGG
172	3.31	GGGA	<b>GC</b>	TTGG
134	3.17	TAGG	<b>GT</b>	TAGG
49	2.91	GGGG	<b>GT</b>	AATT

The table lists, in order, the fold increases in the cleavage intensity after treatment with endonuclease IV. The 5'- and 3'-end-labelled data have been combined. The sequence of the cleavage site is also listed, where the bold region indicates the dinucleotides where the break occurred as well as the flanking tetranucleotide sequences

highest intensity bleomycin sites involved the dinucleotide sequences 5'-GT and to a lesser extent 5'-GC. Table 2 shows the DNA sequences at the 20 most intense bleomycin cleavage sites after endonuclease IV treatment. Again the highest intensity bleomycin sites involved the dinucleotide sequences 5'-GT and 5'-GC. To further investigate this phenomenon, we examined the DNA sequences at the bleomycin cleavage sites with the 20 highest ratios after/before endonuclease IV treatment (Table 3). This analysis revealed that 7 of the top 12 bleomycin cleavage sites were at 5'-GC dinucleotides (Table 3) but before endonuclease IV treatment, only 2 of the top 12 bleomycin cleavage sites were at 5'-GC dinucleotides and these were the eleventh and twelfth ranked sites (Table 1).

Table 4 shows the nucleotide frequencies at bleomycin cleavage sites before and after endonuclease IV treatment and confirmed that 5'-GT dinucleotide sequences (at positions “-1” and “0”) were predominantly cleaved. However, when the after/before endonuclease IV treatment ratios are examined, C nucleotides had a similar frequency at the “0” position as T nucleotides (Table 4), indicating that 5'-GC dinucleotides were similarly present as 5'-GT dinucleotides. Also at the -2 position, C became the predominant

nucleotide and the percentage of G and C at the +1 position increased. This indicates that G and C were preferred at bleomycin-induced abasic sites.

## Discussion

In this work, we described the use of two different fluorescent tags, FAM and PET, to label the 3'- and 5'-ends of DNA fragments, respectively, and to observe their interaction with the DNA cleaving agent bleomycin. The advantage of having the two different end-labelled DNA fragments in the same reaction tube is that they are exposed to exactly the same bleomycin concentration and conditions. This allowed the direct comparison between the two groups without the need for normalising the data due to variance in the concentration of bleomycin.

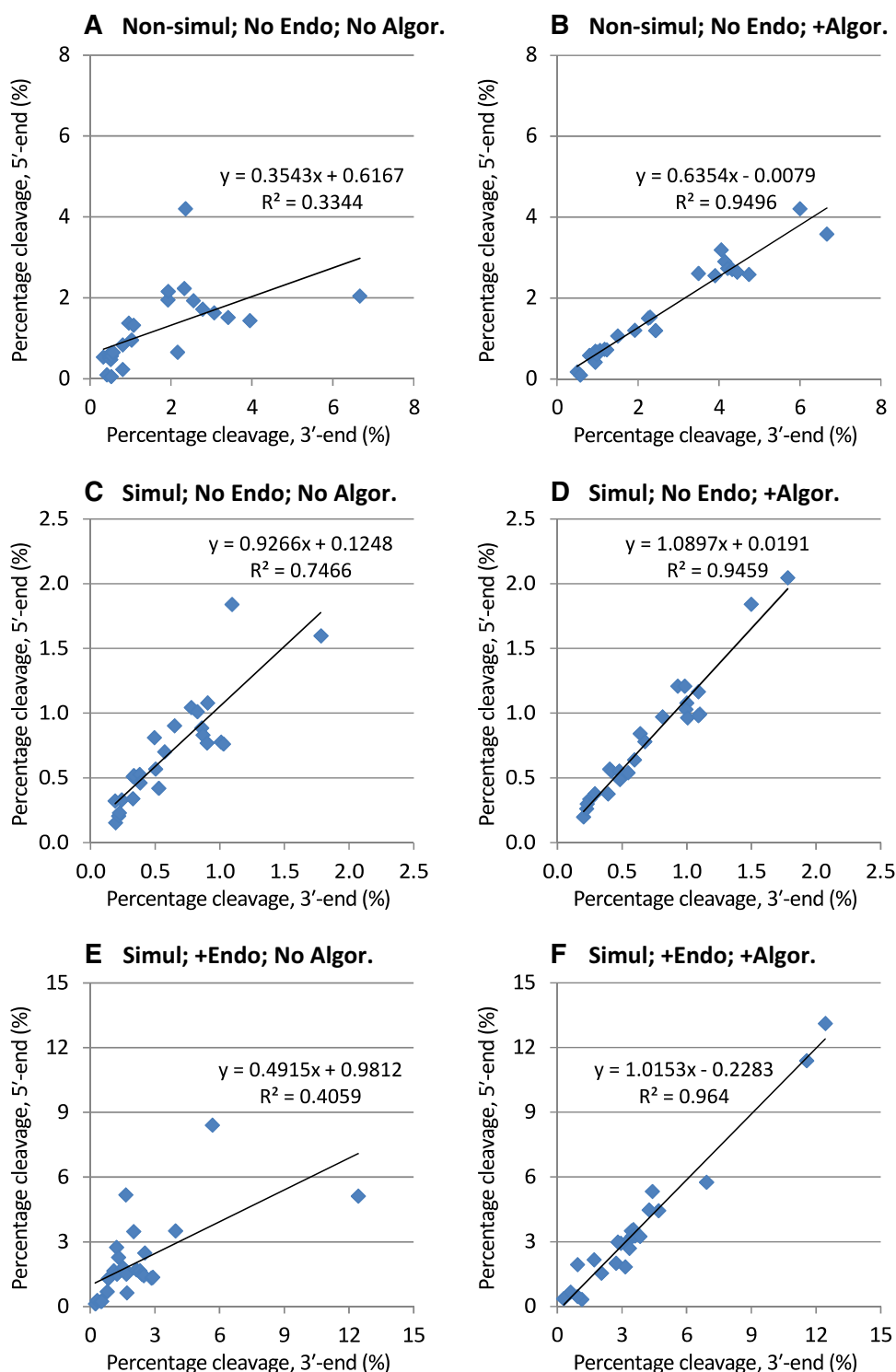
The effect of the correction algorithm was evaluated using  $R^2$  correlation co-efficients comparing the intensity of bleomycin cleavage in DNA labelled at the 3'- or 5'-ends. The results (Fig. 7) showed that application of the correction algorithm substantially increased the  $R^2$  values. This showed the effectiveness of this correction procedure in elimination of most of the end-label bias [34, 35].

As an attempt to further remove end-label bias, a method for simultaneous bleomycin cleavage was developed that labelled 5'- and 3'-ends of DNA with a different fluorescent tag. This permitted both labelled DNAs to be present in the same tube during the bleomycin cleavage reaction. This enabled the slope of the best fitting straight line to be close to a value of one for the simultaneous bleomycin cleavage but was found to be much less than one (0.635) for the non-simultaneous bleomycin cleavage (Fig. 7). The  $R^2$  values were similar with these two conditions. In previous experiments with non-simultaneous cleavage with 5'- and 3'-end-labelled DNA,  $R^2$  values of 0.40, 0.60, 0.90 and 0.95 were achieved [38].

The conditions with the highest  $R^2$  correlation co-efficient (0.964) were simultaneous bleomycin cleavage, with endonuclease IV treatment and application of the correction algorithm. These conditions enable the highest correlation of 5'- or 3'-end labelling. This also implies that the bleomycin cleavage profile is also the most accurate. The correlation co-efficient is not a perfect score of one and hence further improvement is possible, but until a better technique is developed, this procedure is the technique of choice for determining the DNA sequence specificity of a DNA cleaving agent.

The DNA sequence specificity of bleomycin cleavage before endonuclease IV treatment was determined and corresponds to phosphodiester cleavage of DNA fragments (Table 1). The bleomycin specificity was found to be 5'-GT as previously found [13–21].

**Fig. 7** Comparison of bleomycin cleavage intensity with 3'- and 5'-end-labelled DNA. The cleavage frequency of each bleomycin cleavage site, as observed for the 3'- and 5'-labelled ends, was plotted against each other. In panels **a**, **c** and **d**, no correction algorithm was applied; while the correction algorithm was applied in panels **b**, **d** and **f**. Panels **a–d** have not been treated with endonuclease IV; while panels **e** and **f** have been treated with endonuclease IV. The 3'- and 5'-samples in panels **a** and **b** were not treated simultaneously with bleomycin; while panels **c–f** were treated simultaneously with bleomycin. The  $R^2$  values and slope of the best fitting straight line are indicated



Endonuclease IV will cleave DNA at abasic sites [43, 44]. Therefore, any extra cleavage after endonuclease IV treatment is expected to be due to bleomycin-produced abasic sites. Hence, using this endonuclease IV technique, for the first time the DNA sequence specificity of bleomycin-produced abasic sites can be determined. However, there

is a caveat that bleomycin may be producing previously unrecognised types of DNA damage that is recognised by previously undocumented activities of endonuclease IV. Bleomycin produces several DNA damage products and there may be a number of damage products that have not been identified. These unidentified DNA damage products

**Table 4** Relative nucleotide frequency of the ten highest intensity bleomycin cleavage sites

	−5	−4	−3	−2	−1	0	+1	+2	+3	+4
Bleomycin treated only										
G	7	13	59	60	100	0	7	6	51	40
A	24	78	14	0	0	0	35	84	0	14
T	57	9	0	0	0	88	47	0	23	21
C	11	0	27	40	0	12	11	10	27	25
Bleomycin and endonuclease IV treated										
G	12	41	78	56	100	0	12	16	64	55
A	14	48	13	0	0	0	14	84	0	7
T	65	0	0	0	0	91	45	0	20	21
C	9	11	9	44	0	9	29	0	17	18
Ratio (after/before endonuclease IV treatment)										
G	13	47	36	12	100	0	47	37	25	37
A	22	14	14	0	0	0	7	29	15	22
T	35	11	11	11	0	54	0	23	12	12
C	30	28	38	77	0	46	46	10	49	29

The frequency of each nucleotide at bleomycin cleavage sites was quantified. The frequency observed for each nucleotide was normalised to their overall presence in the construct. In addition, the relative frequency of nucleotides flanking the cleavage site was examined. For the purpose of comparison between non-endonuclease IV-treated bleomycin samples (top) and endonuclease IV-treated samples (middle), their respective ten highest intensity cleavage sites were used for this analysis. In addition, a frequency analysis was performed on the top ten sites based on their after/before endonuclease IV ratio (bottom). The −5 −4 −3 −2 −1 0 1 2 3 4 indicates the position of the sequence relative to the cleavage site at “0”

may be recognised by endonuclease IV and endonuclease IV may also cleave at these sites. However, the occurrence of these unidentified DNA damage products is likely to be minor and make a very low contribution to the DNA damage profile after endonuclease IV treatment.

There was an increase in the bleomycin cleavage intensity after endonuclease IV treatment by an average of 4.5-fold (Fig. 6). This implies that there were approximately fourfold more abasic sites produced compared with phosphodiester strand breaks [12]. By use of the after/before endonuclease IV ratio, the sites that are preferentially damaged by bleomycin to give abasic sites were determined. These tended to be 5'-GC and 5'-GT sites rather than the mainly 5'-GT sites for phosphodiester strand breaks.

Bleomycin produces single- and double-strand breaks in the presence of molecular oxygen and abasic damage without molecular oxygen [6]. There was a difference in the DNA sequence preference of bleomycin-induced abasic sites compared with phosphodiester break production. The reaction pathway is different for these two processes with abasic sites being produced without oxygen while phosphodiester break production involves molecular oxygen [6]. The activated form of bleomycin is generated by binding to Fe(II) (ferrous) ions, followed by reduction to form bleomycin-Fe(III)-OOH. This activated form of bleomycin then removes a hydrogen atom from C-4' of the deoxyribose moiety of DNA to form a 4'-radical intermediate. Depending on the availability of oxygen, it can segregate into two

pathways. In the abasic pathway, the 4'-radical intermediate is oxidized to a 4'-carbocation to which water is added and generates a 4'-oxidized abasic site. In the single-strand break pathway, the 4'-radical intermediate reacts with oxygen and a reductant to form a 4'-hydroperoxide which then undergoes a complex series of chemical transformations, and ultimately generates a gapped DNA with 3'-phosphoglycolate and 5'-phosphate ends and a base propenal.

It is likely that in the two reaction mechanisms, the DNA structure and base composition will be important as it interacts with the activated form of bleomycin containing ferrous ions. Hence, in the abasic pathway 5'-GC and 5'-GT dinucleotides appear to be favoured; while for the phosphodiester strand break pathway with molecular oxygen, 5'-GT dinucleotides are preferred. Also G and C were preferred in surrounding sequences at bleomycin-induced abasic sites. In previous sequence specificity studies, endonuclease IV was not utilised and hence bleomycin-induced abasic damage was not part of the analysis and only considered phosphodiester break bleomycin damage.

In general tumours are hypoxic [47, 48] and bleomycin-induced abasic damage is produced when molecular oxygen is lacking. Hence, the bleomycin-induced abasic damage is going to be more important in the context of a hypoxic tumour. The discovery in this paper that the DNA sequence specificity of bleomycin-induced abasic damage is different to phosphodiester strand cleavage implies that a different profile of bleomycin damage will occur in

hypoxic tumour cells. This will invoke a different spectrum of DNA repair pathways that will alter the cellular response to bleomycin chemotherapy compared with phosphodiester strand cleavage. This different response to bleomycin in hypoxic tumour cells could be important in the effectiveness of bleomycin as a cancer chemotherapeutic agent. Hence, this difference in abasic DNA damage should be taken into account when designing novel bleomycin analogues [49, 50].

**Acknowledgments** Support of this work by the University of New South Wales, Science Faculty Research Grant Scheme is gratefully acknowledged.

## References

1. Stoter G, Kaye SB, de Mulder PH, Levi J, Raghavan D (1994) *J Clin Oncol* 12:644–645
2. Einhorn LH (2002) *Proc Natl Acad Sci USA* 99:4592–4595
3. Umezawa H, Maeda K, Takeuchi T, Okami Y (1966) *J Antibiot* 19:200–209
4. Mirabelli CK, Huang CH, Fenwick RG, Crooke ST (1985) *Antimicrob Agents Chemother* 27:460–467
5. Sikic BI (1986) *Cancer Surv* 5:81–91
6. Chen J, Stubbe J (2005) *Nat Rev Cancer* 5:102–112
7. Burger RM (1998) *Chem Rev* 98:1153–1170
8. Burger RM, Berkowitz AR, Peisach J, Horwitz SB (1980) *J Biol Chem* 255:11832–11838
9. Giloni L, Takeshita M, Johnson F, Iden C, Grollman AP (1981) *J Biol Chem* 256:8608–8615
10. Povirk LF, Han YH, Steighner RJ (1989) *Biochemistry* 28:5808–5814
11. Stubbe J, Kozarich JW, Wu W, Vanderwall DE (1996) *Acc Chem Res* 29:322–330
12. Rabow LE, Stubbe J, Kozarich JW (1990) *J Am Chem Soc* 112:3196–3203
13. Takeshita M, Grollman AP, Ohtsubo E, Ohtsubo H (1978) *Proc Natl Acad Sci USA* 75:5983–5987
14. Takeshita M, Kappen LS, Grollman AP, Eisenberg M, Goldberg IH (1981) *Biochemistry* 20:7599–7606
15. D'Andrea AD, Haseltine WA (1978) *Proc Natl Acad Sci USA* 75:3608–3612
16. Kross J, Henner WD, Hecht SM, Haseltine WA (1982) *Biochemistry* 21:4310–4318
17. Mirabelli CK, Ting A, Huang CH, Mong S, Crooke ST (1982) *Cancer Res* 42:2779–2785
18. Murray V, Martin RF (1985) *Nucleic Acids Res* 13:1467–1481
19. Murray V, Tan L, Matthews J, Martin RF (1988) *J Biol Chem* 263:12854–12859
20. Nightingale KP, Fox KR (1993) *Nucleic Acids Res* 21:2549–2555
21. Murray V (2000) *Prog Nucl Acid Res Mol Biol* 63:367–415
22. Murray V, Martin RF (1985) *J Biol Chem* 260:10389–10391
23. Cairns MJ, Murray V (1996) *Biochemistry* 35:8753–8760
24. Kim A, Murray V (2000) *Int J Biochem Cell Biol* 32:695–702
25. Kim A, Murray V (2001) *Int J Biochem Cell Biol* 33:1183–1192
26. Temple MD, Freebody J, Murray V (2004) *Biochim Biophys Acta* 1678:126–134
27. Temple MD, Murray V (2005) *Int J Biochem Cell Biol* 37:665–678
28. Nguyen HTQ, Murray V (2012) *J Biol Inorgan Chem* 17:1209–1215
29. Murray V, Chen JK, Galea AM (2014) *Cell Mol Life Sci* 71:1505–1512
30. Kuo MT, Hsu TC (1978) *Nature* 271:83–84
31. Galea AM, Murray V (2010) *Chem Biol Drug Design* 75:578–589
32. Murray V, Chen JK, Galea AM (2014) *Mutat Res Fundam Mol Mech Mutagen* 769:93–99
33. Paul M, Murray V (2012) *Biomed Chromat* 26:350–354
34. Nguyen TV, Murray V (2012) *J Biol Inorgan Chem* 17:1–9
35. Murray V, Nguyen TV, Chen JK (2012) *Chem Biol Drug Design* 80:1–8
36. Nguyen TV, Chen JK, Murray V (2013) *J Chromat B* 913:113–122
37. Nguyen TV, Murray V (2013) *Biomed Chromat* 27:390–395
38. Chung LH, Murray V (2016) *J Chromat B* 1008:87–97
39. White RJ, Phillips DR (1989) *Biochemistry* 28:4277–4283
40. Gordon LK, Haseltine WA (1980) *J Biol Chem* 255:12047–12050
41. Lobachevsky PN, Martin RF (1996) *Acta Oncol* 35:809–815
42. Chem BiolLobachevsky PN (2000) *Martin RF. Radiat Res* 153:271–278
43. Cunningham R, Saporito S, Spitzer SG, Weiss B (1986) *J Bacteriol* 168:1120–1127
44. Xu YJ, Kim EY, Demple B (1998) *J Biol Chem* 273:28837–28844
45. Murray V, Kandasamy N (2012) *Anti-Cancer Agent Med Chem* 12:177–181
46. Inazuka M, Tahira T, Hayashi K (1996) *Genome Res* 6:551–557
47. Harris AL (2002) *Nat Rev Cancer* 2:38–47
48. Brown JM, Wilson WR (2004) *Nat Rev Cancer* 4:437–447
49. Du L, Sanchez C, Chen M, Edwards DJ, Shen B (2000) *Chem Biol* 7:623–642
50. Huang SX, Feng Z, Wang L, Galm U, Wendt-Pienkowski E, Yang D, Tao M, Coughlin JM, Duan Y, Shen B (2012) *J Am Chem Soc* 134:13501–13509